J Korean Radiol Soc 2006;55:73 - 81

The Usefulness of High-Resolution Three-Dimensional Dynamic MR Imaging with Sensitivity Encoding for Evaluating Extrahepatic Bile Duct Cancer[1]

Young Kon Kim, M.D., Seog Wan Ko, M.D.

Purpose: We assessed the usefulness of high-resolution 3D dynamic MR imaging with sensitivity encoding (mSENSE) for evaluating bile duct cancer.

Materials and Methods: Twenty-three patients with extrahepatic bile duct cancer underwent multiphasic 3D GRE MRI, including two delayed phases without and with mSENSE. The first delayed phases were obtained with volumetric interpolated breath-hold imaging (VIBE) and then the higher in-plane resolution images (320×168) were obtained using mSENSE. The two delayed phase images were compared quantitatively by measuring the signal-to-noise ratio (SNR) of liver and tumor, the liver-visceral fat contrast and the tumor-visceral fat contrast-to-noise ratio (CNR); the two delayed phase images were compared qualitatively by evaluating the sharpness of the hepatic vessels and bile duct, the artifacts and the conspicuity of bile duct cancer.

Results: The quantitative results with mSENSE image were significantly better than those with conventional VIBE. Though the clarity of the intrahepatic vessels and the intrahepatic bile duct, and the artifacts did not differ significantly between the two images ($p > 0.05$), the clarity of the extrahepatic vessels, the extrahepatic bile duct and the bile duct cancer were better on the mSENSE image than on the VIBE ($p < 0.05$).

Conclusion: The higher in-plane resolution 3D GRE image obtained with mSENSE was of a better image quality than the conventional VIBE images. This technique shows promise for use as a comprehensive exam for assessing bile duct cancer.

Index words : Liver, Neoplasms
Magnetic resonance (MR), imaging
Bile ducts, MR
Comparative studies

Liver MR imaging has generally been regarded as the more accurate imaging modality compared with CT imaging (1 - 4). The recent introduction of 3-dimensional, T1-weighted imaging such as the volumetric interpolated breath-hold examination (VIBE) technique has allowed the acquisition of optimum dynamic liver MR imaging with high temporal and spatial resolution, and this type of imaging was previously limited to the 2-dimensional imaging technique (5, 6). However, the 3-dimensional technique using interpolation has limited actual in-plane spatial resolution within about 20 seconds of the breath-hold times relative to CT imaging, and

[1]Department of Diagnostic Radiology, Chonbuk National University Hospital and Medical School
This paper was supported by research funds of Chonbuk National Univeristy in 2005
Received February 8, 2006 ; Accepted April 3, 2006
Address reprint requests to : Young Kon Kim, M.D., Ph D., Department of Diagnostic Radiology, Chonbuk National University Hospital and Medical School, Keumam-dong, JeonJu 560-833, South Korea.
Tel. 82-63-250-2314 Fax. 82-63-272-0481
E-mail: jmyr@dreamwiz.com

shortening of the TE and TR is severely limited when using spectral fat saturation. This 3-dimensional technique might be limited to situations where images showing delicate anatomic detail are needed, for instance, during the evaluation of bile duct cancer and particularly for evaluating the liver hilar area where the portal triads are crowded and complicated by their variable angles (5, 6).

Parallel acquisition technique such as sensitivity encoding (SENSE) has recently been introduced as a method to reduce the scan time with respect to the standard Fourier imaging. This technique is based on the fact that receiver coils with different spatial sensitivity profiles have an encoding effect that is complementary to Fourier preparation and so this allows a reduced acquisition time by means of employing arrays of multiple receiver coils with the resultant decreased number of measured echoes (7, 8). For liver imaging, a few previous studies (9, 10) have demonstrated the efficacy of SENSE MR imaging for detecting hypervascular hepatocellular carcinoma with using multiphasic dynamic imaging. The application of SENSE to dynamic liver MR imaging holds promise for acquiring up-graded images with its higher resolving power relative to conventional imaging by trading the reduced scan time for modification of the scanning parameters, including the image matrix and bandwidth. Therefore, the purpose of this study was to assess the technical feasibility of using mSENSE for acquiring dynamic 3 dimensional-GRE liver imaging with higher in-plane resolution and preserving a sufficient signal-to-noise ratio, and we also wanted to assess its usefulness for evaluating bile duct cancer by comparing it, both quantitatively and qualitatively, with conventional VIBE imaging.

Materials and Methods

Patients

From November 2002 to September 2005, 34 consecutive patients at our tertiary referral hospital who were suspected of having bile duct cancer, based on the previously performed ultrasonography or dynamic helical CT, underwent gadolinium-enhanced multiphasic dynamic MR imaging that included successive acquisition of the equilibrium phase images with and without the integrated parallel acquisition technique. Eleven patients were then excluded from the study due to the lack of histologic confirmation of bile duct wall thickening, even when they were regarded as having bile duct cancer based on the image analysis. Therefore, the remaining 23 patients (14 men and 9 women, mean age: 58 years) were enrolled in this study. A written informed consent was obtained from each patient before they were entered into the study, and this study was approved by the institutional review board of our hospital.

Confirmation of bile duct cancer was made according to surgery in 10 patients and the diagnosis for the remaining 13 patients was based on a combination of the clinical and radiologic findings, including liver MR imaging with MR cholangiopancreatography as well as the cytologic analysis or biopsy that was done via ERCP. According to the morphologic classification of bile duct cancer (11), the bile duct cancer of 18 patients was classified as the infiltrative (periductal) type and remaining five patients had the polypoid (intraductal) type (12). All the bile duct cancers were considered to be located at the extrahepatic bile duct or the hilar area. Among the ten patients with bile duct cancer who underwent surgical resection, seven patients were classified as having Bismuth type I cancer or distal common duct cancer, and the other three were classified as having Bismuth type II cancer. The presence of vascular invasion was not found on both the surgical field and the preoperative images.

MR Imaging

All MR imaging was performed on a 1.5T super-conducting imager (Magnetom Symphony; Siemens, Erlangen, Germany) with using a phased array body coil for signal reception. This system provided a maximum gradient strength of 30 mT/m, with a peak slew rate of 125 mT/m/msec. All the images were obtained in the axial plane. Before the gadolinum-enhanced dynamic MR imaging was performed, the axial fat-suppressed T1-weighted fast low-angle shot (FLASH) sequences were obtained with the following parameters: a TR/TE of 159/2.6, a flip angle of 70 °, a matrix of 120×256; a 6-mm slice thickness, a 10% intersection gap, a 35-40 cm field of view and a scan time of 37 sec. Dynamic imaging was performed after the administration of gadobenate dimeglumine (Gd-BOPTA; MultiHance, Bracco, Milan, Italy) at a dose of 0.1 mmol/kg, and this was followed by 20-mL of saline flush. Determining the scan delay for timing the image acquisition was achieved by a test bolus technique in which 1mL of gadobenate dimeglumine was injected along with a saline flush; the vessel of interest (the abdominal aorta) was then scanned approximately once per second. The T1-

weighted images for the arterial phase (20 - 35 sec) and portal phase (45 - 60 sec) imaging were obtained by performing three-dimensional Fourier transform gradient echo imaging (volumetric interpolated breath-hold examination, VIBE: Siemens, Erlangen, Germany) with using the following parameters: a TR/TE of 3.6/1.6, a flip angle of 12 °, a bandwidth of 490Hz/Px and a 75% rectangular field of view of 32 - 35×24 - 26 cm (5, 6). 256 encoding steps were used for the read-direction. 67% partial Fourier sampling was done for the phase-encoding direction and then an initial matrix of 256×120 data points was interpolated by zero filling to a matrix of 512 ×240. So, the initial in-plane resolution of 1.4×2.2 mm2 or less was interpolated to a pixel size of 0.7×1.1 mm2 or less. For the selection-select or the partition direction, data sampling was done at 70% to produce 70 - 72 partitions and an effective slice thickness of 2.3 mm.

Two successive images were obtained for the dynamic equilibrium phases with delays of 180 sec after the injection of contrast media: the first equilibrium phases were acquired using the VIBE technique with the same parameters as the dynamic arterial and portal phases. Immediate after the first equilibrium phase, the second equilibrium phases were acquired with mSENSE and using the following parameters: a TR/TE of 5.3/2.6, a flip angle of 12 °, a bandwidth of 300Hz/Px, a matrix of 320 (read)×168 (phase)×46-48 (partition), and an effective slice thickness of 3.0 mm. A 75% rectangular field of view of 320-350×240 - 263 mm^2 and an image matrix of 320×168 yielded an in-plane resolution of 1.1×1.6 mm^2 or less. Interpolation was used for only the partition direction by acquiring the initial 70% sampling. A combination of a phased array body coil and a spine array coil with eight coil elements was used for the parallel acquisition technique, and mSENSE with a reduction factor of two was applied in an in-plane phase encoding direction for the 3D-dynamic imaging. mSENSE allowed acquisition of the folded images in each of the eight receiver channels by reducing the k-space sampling and then unwrapping them in the reconstruction process from a reference scan (8). Twenty-four effective reference lines were used for each receiver channel. The acquisition time was the same (17 - 19 seconds) for each dynamic phase image, including the equilibrium phase image of the high-resolution image and the conventional VIBE.

Image Analysis

Qualitative Analysis: All the images were jointly evaluated by two gastrointestinal radiologists (Y. K. K and S. W. K) who were well experienced in interpreting MR liver imaging in their daily clinical practice. Qualitative image analysis was performed both separately and independently with the quantitative measurements. The two observers were blinded to the patients' histories and the sequence information. Two images were randomly presented to minimize any learning bias. Discrepancies on interpretation were resolved by means of a consensus reading. The two observers subjectively rated each sequence for the clarity of the hepatic vessels (the intrahepatic and extrahepatic portal vein and hepatic artery) and the intrahepatic and extrahepatic bile duct, any artifacts and the conspicuity of the bile duct cancer. The overall image quality and clarity of the vessels, the bile duct and the bile duct cancer was based on the following grading scale: unacceptable was 1, poor was 2, fair was 3, good was 4 and excellent was 5. The presence of artifacts was rated using the following grading scale: 1 was absent, 2 was mild, 3 was moderate and 4 was severe.

Quantitative Analysis: Quantitative image analysis was performed by measuring the signal intensity of the liver, the tumors, the visceral fat and the standard deviation of the background noise with using the operator-defined regions of interest (ROIs) for each image by the two reviewers. For minimizing errors, we obtained an average of three measurements by each reviewer. For the signal intensities of the liver and visceral fat, ROIs were drawn on the same location on each image that was devoid of large blood vessels. When the bile duct cancer was too small to place a ROI, then the image was magnified as much as three times. The standard deviation (SD) of the background noise was measured along the phase-encoding direction outside the body just ventral to the right anterior abdominal wall, and this included any respiratory or motion-related artifacts. The shape and size of the ROIs were, as much as possible, identical for all images. The signal-to-noise ratio (SNR) of the liver and the tumor, the liver-to-visceral fat contrast and the tumor to visceral fat contrast-to-noise ratio (CNR) were calculated from the signal intensity of the liver, the tumors, the visceral fat and the SD of the background noise according to the following formulas:

SNR = signal intensity of liver (lesion)/SD of background noise

Tumor-to-visceral fat CNR = {signal intensity of tumor-signal intensity of visceral fat}/SD of the background noise

Liver-to-visceral fat contrast = {signal intensity of liv-

er - signal intensity of visceral fat}/SD of the background noise

Statistical Analysis

The qualitative and quantitative values were reported as means±SDs. The statistical significance of the quantitative data for the signal intensities of the liver parenchyma and the tumor, the SNR of the liver parenchyma and the tumor, the liver-to-visceral fat contrast and the tumor-to-visceral fat CNR were determined using repeated measures of analysis of variance testing (ANOVA), and the differences between the groups were compared using the paired t test. In addition, the statistical significance of the qualitative data for the clarity of the hepatic vessel and bile duct, and also the conspicuity of the bile duct cancer and the artifacts was determined using the Wilcoxon signed rank test. A p value less than .05 was considered statistically significant. The statistical analyses were performed using SPSS 8.0 computer software (SPSS Inc., Chicago, IL, USA).

Results

The quantitative results for the mean SNR of the liver parenchyma and tumor, as well as the liver-to-visceral fat contrast and the tumor-to-visceral fat CNR for each image, are shown in Table 1. The mean SNRs of the liver and the liver?to-visceral fat contrast on the mSENSE images were significantly higher than those on the conventional VIBE images (mean SNR of the liver: 70.8± 8.2 vs 62.4±10.0, respectively, $p=0.013$; mean SNR of the liver-to-visceral fat contrast: 58.4±7.9 vs 44.0±9.4, respectively, $p=0.0001$). The mean SNR of the tumor and the tumor-to-visceral fat CNR on the mSENSE images were also significantly higher than those on the conventional VIBE images (mean SNR of the tumor: 276.1±44.9 vs 242.9±34.9; the tumor-to-visceral fat CNR: 264.2±45.2 vs 223.1±36.4, $p=0.0001$, respectively). Although the mean signal intensity of the liver parenchyma and tumor on the mSENSE images were higher than those on the conventional VIBE images (mean signal intensity of liver: 116.8±10.1 vs 91.1± 11.7; mean signal intensity of tumor, 458.3±66.4 vs 352.9±47.0, $p=0.0001$, respectively), the mean signal intensity of visceral fat was lower on the mSENSE images than on the conventional VIBE images (20.3±3.4 vs 26.9 ±3.5, $p=0.0001$, respectively).

The results of the qualitative analysis are shown in Table 2. Although the sharpness of the intrahepatic vessel (3.9±0.3 vs 3.8±0.4, respectively) and the intrahepatic bile duct (3.9±0.4 vs 3.8±0.4, respectively) did not differ significantly between the two images ($p=0.83$) (Fig. 1), the sharpness of the extrahepatic portal vein and the hepatic artery (3.8±0.4 vs 3.2±0.4, respectively) as well as for the extrahepatic bile duct (3.9±0.4 vs 3.2± 0.5, respectively) was significantly better on the mSENSE image than on the conventional VIBE image ($p=0.0001$) (Fig. 2). In addition, the conspicuity of the bile duct cancer was significantly better on the mSENSE image than on the conventional VIBE image (3.9±0.3 vs 3.6±0.5, respectively, $p=0.014$) (Fig. 2, 3). Although minimal band-like aliasing artifacts were seen on most of the mSENSE images, there was no significant difference in the artifacts between the two images (3.8±0.5 vs 3.9±0.4, respectively, $p=0.31$) (Fig. 2).

Table 1. Comparison of the Quantitative Analysis: Higher In-Plane Resolution Dynamic Image with Sensitivity Encoding (mSENSE) vs the Volumetric Interpolated Breath-Hold Examination (VIBE)

	SNR of the Liver	SNR of Tumor	Liver-Visceral fat Contrast	Tumor-Visceral fat CNR
mSENSE Image	70.8±8.2*	276.1±44.9*	58.4±7.9*	264.2±45.2*
VIBE	62.4±10.0	242.9±34.9	44.0±9.4	223.1±36.4

Note. - Data are presented as means±SDs. * There were significant differences between the two images ($p<0.05$).
SNR = signal-to-noise ratio, CNR = contrast-to-noise ratio.

Table 2. Comparison of the Qualitative Analysis: Higher In-Plane Resolution Dynamic image with Sensitivity Encoding (mSENSE) vs the Volumetric Interpolated Breath-Hold Examination (VIBE)

	Sharpness of the Bile Duct		Sharpness of the Vessel		Conspicuity of	Artifact
	Intrahepatic	Extrahepatic	Intrahepatic	Extrahepatic	The Bile Duct Cancer	
mSENSE Image	3.9±0.4	3.9±0.4*	3.9±0.3	3.8±0.4*	3.9±0.3*	3.9±0.4
VIBE	3.8±0.4	3.2±0.5	3.8±0.4	3.2±0.4	3.6±0.5	3.8±0.5

Note. - Data are presented as means±SDs. * There were significant differences between the two images ($p<0.05$).

Discussion

Obtaining the highest resolving power to discriminate subtle disease might be an ultimate goal of the various image modalities, and this could be achieved with higher spatial resolution, an improved signal-to-noise ratio and better object contrast (13). From that point of view, there have been a few reports demonstrating the usefulness of dynamic liver MR imaging with employing phased array multicoils and higher image matrices (512 ×256 [frequency x phase-encoding matrices]) for evaluating hepatocellular carcinoma (14, 15). However, the technique used in those previous studies was a 2D GRE sequence that required a relatively long-breath holding time (26 seconds for 10 images) and a thick section of 8 to 10 mm, and this may obscure small hepatic lesions according to the partial volume averaging effect. Using the VIBE technique for the dynamic images in our study has several advantages over the 2-D GRE technique such as thinner sections, no gaps, fat saturation, higher SNR, comparable image contrast and the generation of MR angiography based on the isotropic voxels (5, 6); most of these things are possible by shortening the im-

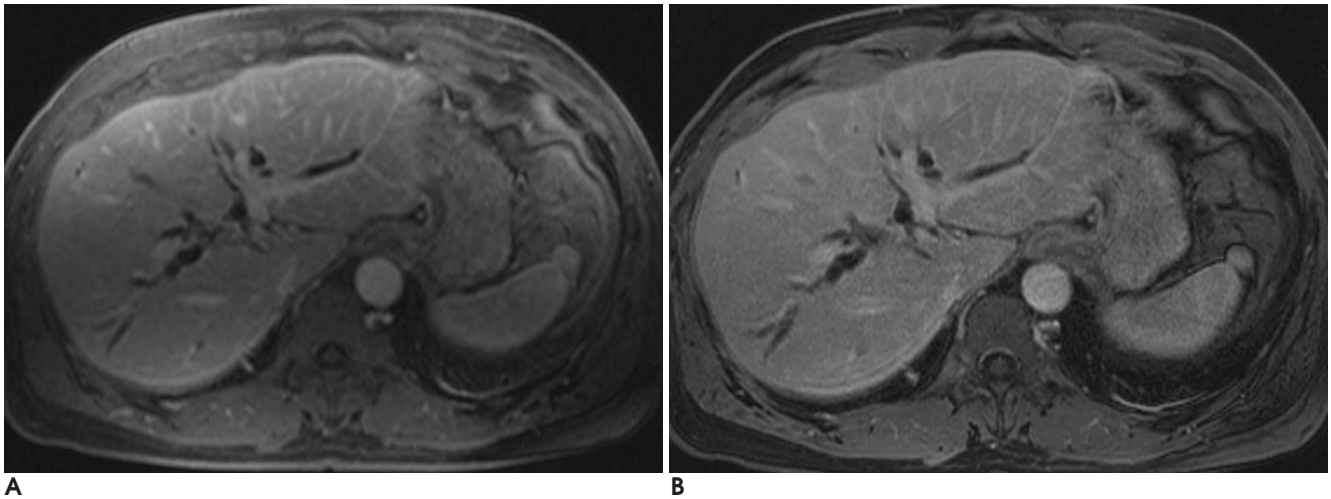

A B

Fig. 1. A 63-year-old man with biliary dilatation due to common duct stones.
The three-dimensional dynamic delayed phase MR images obtained with using a volumetric interpolated breath-hold examination (VIBE) without mSENSE (**A**) and with mSENSE and high-resolution (**B**). The sharpness of the intrahepatic vessels and the dilated intrahepatic bile duct did not significantly differ between the two images.

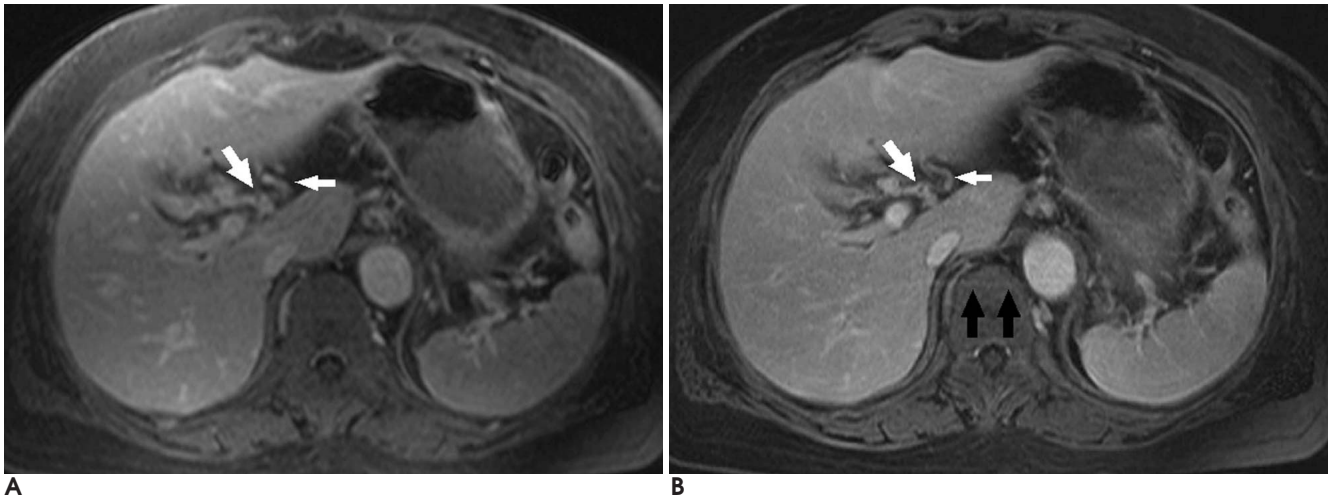

A B

Fig. 2. A 61-year-old man with surgically confirmed common duct cancer.
The three-dimensional dynamic delayed phase MR images obtained with using a volumetric interpolated breath-hold examination (VIBE) without mSENSE (**A**) and with mSENSE and high-resolution (**B**). A small bile duct cancer (large arrow) and the adjacent hepatic artery (small arrow) are more clearly depicted on the mSENSE image than on the conventional VIBE sequence. Note the minimal band-like aliasing artifact (black arrows) in the mSENSE image that did not influence the overall image quality.

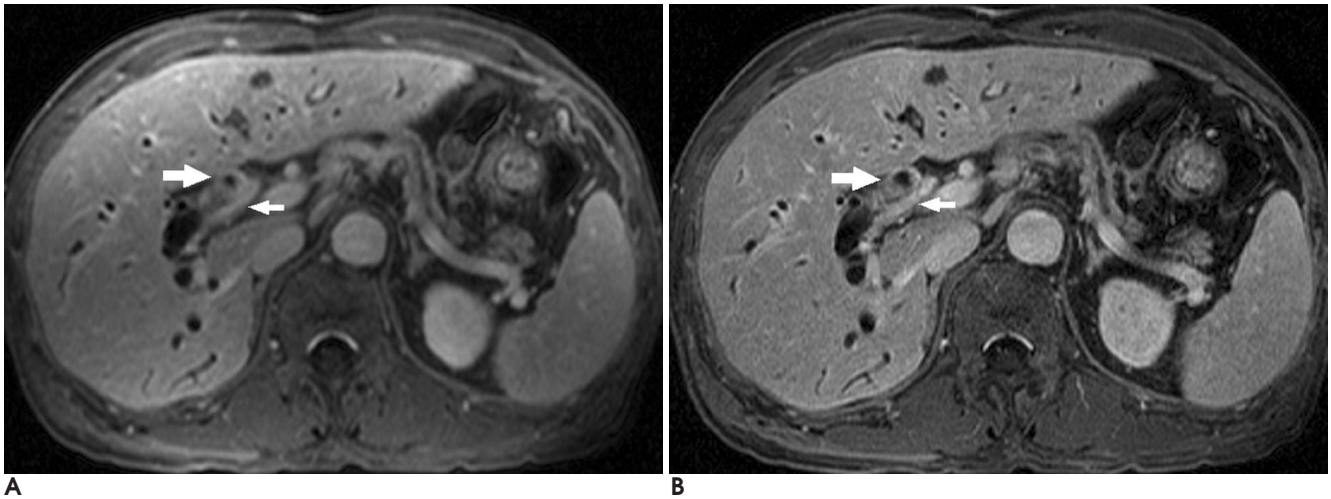

A B

Fig. 3. A 60-year-old man with the surgically confirmed common duct cancer.
The three-dimensional dynamic delayed phase MR images obtained with using a volumetric interpolated breath-hold examination (VIBE) without mSENSE (**A**) and with mSENSE and high-resolution (**B**). The conspicuity of the small bile duct cancer (large arrow) and the adjacent hepatic artery (small arrow) is better on the mSENSE image than on the conventional VIBE sequence.

age acquisition time as well as increasing the resolution by performing interpolation. However, breath-hold times exceeding 20 seconds limit the VIBE technique 's spatial resolution because of the time-consuming phase-encoding steps of two-directions with applying spectral fat saturation. Furthermore, although zero filling interpolation is used for VIBE, the actual in-plane matrix is defined as 256×120, which is inferior to CT images, and so might be limited to situations where an imaging showing delicate anatomic detail is needed. Therefore, to overcome this relatively lower spatial resolution of the popularly used 3D GRE image compared to the CT imaging, a faster image acquisition technique is inevitably needed and the introduction of a parallel acquisition technique such as mSENSE could be the solution for this problem.

For acquiring the optimized, highest-resolution liver MR imaging, the concerns for the SNR and CNR as well as a reasonable image acquisition time should be considered. For achieving the higher in-plane resolution imaging in our study, we choose the highest possible matrix size of 320×168 (frequency×phase-encoding matrices) without zero filling interpolation, while maintaining an adequate image acquisition time and the SNR and CNR. The 3D dynamic image with frequency encoding steps of 512, in our experience, showed grainy images with a remarkable drop of the SNR as well as the CNR relative to the conventional VIBE technique. In spite of the increased image matrices, the acquisition time of the mSENSE image was the same as the conventional VIBE thanks to the application of mSENSE. However, theoretically, by reducing the number of measured echoes and the non-optimum weighting of the arrayed coil elements, the SNR of the mSENSE images is decreased according to the square-root of the acquisition time, and it is inversely proportional or at least equal to the square root of the reduction factor (8). Furthermore, the CNR drop was also anticipated by decreasing the voxel size in the mSENSE image (13, 16). In actual clinical practice, Vogt et al. (17) have recently demonstrated that the SNR and CNR of the 3D dynamic imaging obtained with the parallel acquisition techniques such as Generalized Autocalibrating Partially Parallel Acquisition (GRAPPA) and mSENSE were decreased up to 35% in comparison to the unaccelerated VIBE. However, Vogt and colleagues used only four coil array elements, which was different from the eight coil elements in our study. This could be one possible reason for higher SNR of the mSENSE image. Also, a low bandwidth (490→300 Hz/Px) was used to compensate for the SNR penalty as well as the CNR penalty with using mSENSE and also the increased in-plane resolution in our study. (18). However, the thinner partition of the conventional VIBE (2.3 mm→3.0 mm) was inevitably sacrificed for the SNR penalty, as well as for maintaining the same image acquisition time as the conventional VIBE. As a result, on the quantitative analysis of this study, the SNR of liver and tumor on the mSENSE image was significantly higher than those on the conventional VIBE sequence. In addition, the liver-to-visceral fat contrast and the tumor-to-visceral fat CNR on the mSENSE image were significantly higher than those on the conventional

VIBE, and this resulted from the marked fat suppression as well as the increased SNR of liver on the mSENSE image (Fig. 3). We could not find a clear explanation for the marked fat suppression with the mSENSE image, though this might be explained by a better spectral separation at the longer TE and the fact that at the longer TE, fat and water protons are at an opposed phase in contrast to being in-phase at the TE of the conventional VIBE sequence.

On qualitative analysis of our study, the sharpness of the intrahepatic vessels and the intrahepatic bile duct did not differ significantly between the two images, although the sharpness of the extrahepatic portal vein, the hepatic artery and the extrahepatic bile duct as well as the conspicuity of the bile duct cancer were significantly better on the mSENSE image than on the conventional VIBE. This stands in contrast to the results of a study by Vogt et al. (17) that demonstrated poorer quantitative and qualitative results of the 3D dynamic image with the parallel acquisition technique than that for the unaccelerated VIBE when the same image parameters were used for both techniques. The enhanced clarity of the extrahepatic bile duct, the hepatic artery and the portal vein as well as bile duct cancer on the mSENSE image could be explained by the optimized SNR and CNR that resulted from the best possible combination of the highest image matrix and bandwidth. In terms of image artifacts, we observed only minimal fold-over aliasing artifacts on most of the mSENSE images, which didn't degrade the overall image quality and it didn't interfere with the evaluation of the bile duct and vessels. This was a milder degree of aliasing artifacts than was expected and was shown in a study by Vogt et al. (17), and this could be attributed to the mSENSE algorithm that we used rather than the GRAPPA algorithm; furthermore, the eight arrayed coil elements we used compared with the four element in the study by Vogt et al. (17) were beneficial for minimizing the aliasing artifacts.

Our study demonstrated that the application of mSENSE makes it possible to acquire upgraded 3-dimensional dynamic MR images that have higher in-plane spatial resolution and better contrast by trading off saving time for a larger matrix and a lower bandwidth, relative to the conventional VIBE. Additionally, the positive impact of the improved spatial resolution on the image quality as well as excellent delineation of bile duct cancer was shown on the mSENSE imaging. We suggest that for the cases of patients who are able to hold their breaths for acquiring the conventional VIBE sequence, applying mSENSE for dynamic liver MR imaging should be weighed according to acquiring high quality imaging relative to the conventional unaccelerated image, and not simply for reducing the data acquisition time, regardless of the image quality and any concerns about the SNR and CNR.

This study has some limitations. First, the order for acquiring the two dynamic equilibrium phase images was the same for all our study subjects, i.e., the successive acquisition of the first conventional VIBE image and then the second mSENSE image. However, we believe that there was an insignificant difference of signal intensity between the two successive equilibrium phase images that were acquired at more than 3 min after the injection of contrast media (19). Nevertheless, the SNR of the late equilibrium phase image with higher-resolution was significantly higher than that of the early conventional VIBE image. Second, surgical confirmation was not done in all 23 patients with bile duct cancer. The 10 patients with bile duct cancer who had surgical resection performed were classified as Bismuth type I or II without them having any evidence of vascular invasion or adjacent liver parenchyma on both the preoperative image analysis and surgery, so any precise comparison between the two dynamic equilibrium phases for determining the resectability could not be performed. Third, the 3.0 mm section thickness on the high-resolution image was slightly thicker than the 2.3 mm of the conventional VIBE technique. Radiologic assessment of the bile duct cancer is influenced by the resolution in multiple planes and not just by the in-plane resolution, so reformat images such as the coronal and sagittal planes should be evaluated for both the conventional VIBE and mSENSE imagings. However, the aim of our study was not making comparison between the dynamic MR imaging with higher longitudinal resolution and the dynamic MR imaging with higher in-plane resolution, but we only demonstrated the application of mSENSE to 3D dynamic MR imaging to acquire images of a higher quality. The acquisition of the thinner slice higher-resolution image could be possible with some modification of the parameters used in our study because the SNR and CNR in the original VIBE are already in an acceptable range. Further, the use of MR equipment having a higher gradient strength makes it possible to acquire a thinner section image than that obtained of our study. Last, a phase matrix of 168 might be somewhat small as a high resolution image relative to conventional VIBE. However, in our study sample, the mean body weight and height

were 63.3 kg (range: 47 - 75 kg), and 166 cm (range: 153 - 173 cm); thus, it may not be possible to generalize the results of our study to the North American population where the average body mass index is expected to be higher.

In conclusion, the higher in-plane resolution 3-dimensional GRE image with mSENSE showed superior image quality than did the conventional VIBE image with using the same acquisition time, and this technique shows promise for conducting a comprehensive exam for the assessment of biliary obstructive disease.

References

1. Choi D, Kim SH, Lim JH, Lee WJ, Jang HJ, Lee SJ, et al. Preoperative detection of hepatocellular carcinoma: ferumoxides-enhanced MR imaging versus combined helical CT during arterial portography and CT hepatic arteriography. *AJR Am J Reontgenol* 2001;176:475-482
2. Hagspiel KD, Neidl KF, Eichenberger AC, Weder W, Marincek B. Detection of liver metastases: comparison of superparamagnetic iron oxide-enhanced and unenhanced MR imaging at 1.5 T with dynamic CT, intraoperative US, and percutaneous US. *Radiology* 1995;196:471-478
3. Bartolozzi C, Donati F, Cioni D, Crocetti L, Lencioni R. MnDPDP-enhanced MRI vs dual-phase spiral CT in the detection of hepatocellular carcinoma in cirrhosis. *Eur Radiol* 2000;10:1697-1702
4. Kang BK, Lim JH, Kim SH, Choi D, Lim HK, Lee WJ, et al. Preoperative depiction of hepatocellular carcinoma: ferumoxides-enhanced MR imaging versus triple-phase helical CT. *Radiology* 2003; 226:79-85
5. Rofsky NM, Lee VS, Laub G, Pollack MA, Krinsky GA, Thomasson D, et al. Abdominal MR imaging with a volumetric interpolated breath-hold examination. *Radiology* 1999;212:876-884
6. Lee VS, Lavelle MT, Rofsky NM, Laub G, Thomasson DM, Krinsky GA, et al. Hepatic MR imaging with a dynamic contrast-enhanced isotropic volumetric interpolated breath-hold examination: feasibility, reproducibility, and technical quality. *Radiology* 2000;215:365-372
7. Madore B, Pelc NJ. SMASH and SENSE: experimental and numerical comparisons. *Magn Reson Med* 2001;45:1103-1111
8. Pruessmann KP, Weiger M, Scheidegger MB, Boesiger P. SENSE: sensitivity encoding for fast MRI. *Magn Reson Med* 1999;42:952-962
9. Yoshioka H, Takahashi N, Yamaguchi M, Lou D, Saida Y, Itai Y. Double arterial phase dynamic MRI with sensitivity encoding (SENSE) for hypervascular hepatocellular carcinomas. *J Magn Reson Imaging* 2002;16:259-266
10. Takahashi N, Yoshioka H, Yamaguchi M, Saida Y, Itai Y. Accelerated dynamic MR imaging with a parallel imaging technique for hypervascular hepatocellular carcinomas: usefulness of a test bolus in examination and subtraction imaging. *J Magn Reson Imaging* 2003;18:80-89
11. Bismuth H, Corlette MB. Intrahepatic cholangioenteric anastomosis in carcinoma of the hilus of the liver. *Surg Gynecol Obstet* 1975;140:170-178
12. Lee WJ, Lim HK, Jang KM, Kim SH, Lee SJ, Lim JH, et al. Radiologic spectrium of cholangiocarcinoma: emphasis on unusual manifestations and differential diagnoses. *Radiographics* 2001; 21:S97-S116
13. Bradley WG Jr, Kortman KE, Crues JV. Central nervous system high-resolution magnetic resonance imaging: effect of increasing spatial resolution on resolving power. *Radiology* 1985;156:93-98
14. Fujita T, Ito K, Honjo K, Okazaki H, Matsumoto T, Matsunaga N. Detection of hepatocellular carcinoma: comparison of T2-weighted breath-hold fast spin-echo sequences and high-resolution dynamic MR imaging with a phased-array body coil. *J Magn Reson Imaging* 1999;9:274-279
15. Kanematsu M, Hoshi H, Murakami T, Itoh K, Hori M, Kondo H, et al. Detection of hepatocellular carcinoma: comparison of low- and high-spatial-resolution dynamic MR images. *AJR Am J Reontgenol* 1999;173:1207-1212
16. Hart HR Jr, Bottomley PA, Edelstein WA, Karr SG, Leue WM, Mueller O, et al. Nuclear magnetic resonance imaging: contrast-to-noise ratio as a function of strength of magnetic field. *AJR Am J Reontgenol* 1983;141:1195-1201
17. Vogt FM, Antoch G, Hunold P, Maderwald S, Ladd ME, Debatin JF, et al. Parallel acquisition techniques for accelerated volumetric interpolated breath-hold examination magnetic resonance imaging of the upper abdomen: assessment of image quality and lesion conspicuity. *J Magn Reson Imaging* 2005;21:376-382
18. Mitchell DG, Vinitski S, Rifkin MD, Burk DL Jr. Sampling bandwidth and fat suppression: effects on long TR/TE MR imaging of the abdomen and pelvis at 1.5T. *AJR Am J Reontgenol* 1989;153: 419-425
19. Heiken JP, Brink JA, McClennan BL, Sagel SS, Forman HP, DiCroce J. Dynamic contrast-enhanced CT of the liver: comparison of contrast medium injection rates and uniphasic and biphasic injection protocols. *Radiology* 1993;187:327-331

J Korean Radiol Soc 2006;55:73 - 81

대한영상의학회지 2006;55:73 - 81

간외 담관암 평가에 있어서 Sensitivity Encoding을 이용한 고해상도 3차원 역동기 자기공명영상의 유용성[1]

[1]전북대학교병원 영상의학과

김 영 곤 · 고 석 완

목적: Sensitivity encoding (mSENSE) 기법을 이용한 고해상도 3차원 역동기 자기공명영상의 간외 담관암 평가의 유용성을 알아보고자 하였다.

대상과 방법: 간외 담관암으로 volumetric interpolated breath - hold imaging (VIBE) 기법의 가돌리늄 조영증강영상을 시행한 23명의 환자를 대상으로 하였다. 역동기 영상중 지연기는 고식적인 VIBE 기법과 mSENSE를 이용해 해상도를 높인 (320×168) 영상 두 가지를 연이어서 얻었다. 정량적 분석으로 두 개의 지연기 영상 간의 간 과종양에 대한 신호대 잡음비와, 간과 종양 - 내장지방과의 대조도를 얻어 비교하였고 정성적 분석으로 간혈관, 담관, 인공물, 담관암의 명확도에 대하여 비교 분석하였다.

결과: mSENSE 기법을 이용한 영상의 정량적 분석에 대한 결과가 고식적인 VIBE 기법에 비해 통계적으로 우수하였다. 간내혈관 과 간내담도, 인공물에 대한 정성분석의 결과는 양자간에 의미있는 차이를 보이지 않았으나 ($p > 0.05$), 간외혈관과 간외담도, 담관암의 명확도는 mSENSE 기법을 이용한 영상이 고식적인 VIBE 기법에 비해서 우수하였다 ($p < 0.01$).

결론: mSENSE 기법을 이용한 고해상도 3차원 역동기 자기공명영상은 고식적인 VIBE 기법에 비해 더 나은 영상화질을 보여 주었고 이는 담관암 환자의 평가에서 유용하리라 생각된다.